The Impact of Solar Variability on Climate

Joanna D. Haigh

A general circulation model that simulated changes in solar irradiance and stratospheric ozone was used to investigate the response of the atmosphere to the 11-year solar activity cycle. At solar maximum, a warming of the summer stratosphere was found to strengthen easterly winds, which penetrated into the equatorial upper troposphere, causing poleward shifts in the positions of the subtropical westerly jets, broadening of the tropical Hadley circulations, and poleward shifts of the storm tracks. These effects are similar to, although generally smaller in magnitude than, those observed in nature. A simulation in which only solar irradiance was changed showed a much weaker response.

The idea that variation in solar activity may affect the climate has been discussed as early as 1795, when Herschel (*1*) proposed such a possibility. Since that time, numerous studies have shown statistical correlations between various meteorological parameters and different measures of solar activity. To date it has not proved possible, however, to simulate these apparent changes with the use of atmospheric general circulation models and realistic changes in solar radiative forcing. Using a 36-year time series of Northern Hemisphere temperatures derived from satellite data, Labitzke and van Loon [henceforth LvL; (*2*, *3*)] showed significant correlations between solar activity and 30-hectopascal (hPa) geopotential height, especially in mid-latitudes. Using temperature profiles from radiosonde data, LvL also found a consistent warming of the mid-latitude troposphere at solar maximum relative to solar minimum. Other evidence has concerned the positioning of the mid-latitude storm tracks. Brown and John (*4*) suggested that as storms crossing the North Atlantic reach land, they tend to follow one of two routes—a northern path across Scandinavia or a southern path across the Mediterranean—and that these paths tend to converge at periods of higher solar activity.

The variation in the sun's total energetic output, as determined over time scales for which reliable climatic data are available, is <0.1% (corresponding to an irradiance of ~1 W m^{-2} outside the atmosphere, or 0.2 W m^{-2} averaged over Earth's surface) between periods of maximum and minimum activity over the 11-year solar cycle. It is not clear how such small changes can be responsible for the apparent fluctuations in climate. The magnitude of the variation of solar radiation is, however, a strong function of wavelength, with the highest amplitude in the ultraviolet (UV) range. Wavelengths shorter than 400 nm, which contribute ~9% to the total irradiance, provide ~32% of the change (*5*). Therefore, solar variability can influence the structure of the middle atmosphere through modification of photochemical dissociation rates and the subsequent effect on the chemistry of ozone and other gases (*6*).

Space and Atmospheric Physics, Blackett Laboratory, Imperial College of Science, Technology and Medicine, London SW7 2BZ, UK.

Global modeling studies of the impact of solar variability have either used increases in UV radiation to simulate the middle atmosphere and deduce subsequent dynamical effects on the troposphere (*7*, *8*) or used spectrally flat increases in total solar irradiance to study the impact of such a change in radiative forcing on climate (*9*). None of these studies included a modulation of stratospheric ozone as part of the solar impact [thus, they misrepresented the vertical and latitudinal distribution of the change in irradiance (*10*)], and most of them used unrealistically large changes in radiative forcing. Nevertheless, these studies have been successful in simulating some aspects of the observed phenomena, and they have illuminated the problem by suggesting that particular changes in the hydrological cycle, in planetary wave activity, or in the mean circulation of the atmosphere may play a role in enhancing the initial direct radiative effects.

In the present study, an attempt was made to simulate the impact on the lower atmosphere of changes in solar radiation corresponding to extremes of the 11-year cycle, with the use of realistic assumptions concerning the magnitude of the change in irradiance, a crude representation of the wavelength dependence of the solar variability, and inclusion of the modulation of lower stratospheric ozone. The simulation model was based on the European Centre for Medium Range Weather Forecasting spectral model, which was developed within the UK Universities' Global Atmospheric Modelling Programme (UGAMP). A horizontal resolution of approximately 2.8° latitude by 2.8° longitude and 19 vertical steps up to 10 hPa (~30 km) were used; the time step was 30 min. Sea surface temperatures were fixed, whereas land surface temperatures and soil moisture were determined by a three-layer soil model. The radiation scheme was that of Morcrette (*11*). [See Slingo *et al.* (*12*) for more details about this model.]

Three 1260-day runs of the model were performed, all in perpetual January mode. In this mode the solar declination does not vary, but there is a full diurnal cycle; this allows for a detailed study of January conditions without the need for several years' integration. Such experiments incorporate the "natural" variability of the season but are loosely constrained by the sea surface temperatures. An initial period of 180 days was used for equilibration of the system; the results were averaged over the remaining 1080 days. The first model run, run I, represents conditions prevalent when the sun is at minimum activity during its 11-year cycle. The second, run IIa, represents solar maximum in terms of increases in both solar irradiance and stratospheric ozone. In run IIb, the solar irradiance was increased as in run IIa, but the ozone was maintained as in run I. The shortwave radiation scheme used in the model has two spectral intervals, one covering the UV and visible range and one covering the near-infrared range; it has been assumed that almost all the variation occurs within the first spectral interval (*13*) (Table 1). Because absorption in the first interval is only by ozone, its contribution will be almost entirely in the stratosphere, whereas absorption in the second interval is mainly by water vapor and carbon dioxide, which are more important in the troposphere. It follows that the changes shown in Table 1 will have little direct radiative impact on the troposphere. Moreover, although ~55% of the change in incident radiation between solar maximum and solar minimum reaches the surface (88% for run IIb), the model used here has fixed sea surface temperatures, such that the potential for any indirect effect through heating of the surface is also small (especially in January, when the greatest effect of land surface temperatures is in the Southern Hemisphere, which has little land cover). The change in total irradiance between so-

Table 1. Solar irradiance specified in the two wavelength intervals and totals for the model runs at solar minimum (run I) and solar maximum (runs IIa and IIb).

Solar irradiance	Wavelength (μm) 0.25 to 0.68	Wavelength (μm) 0.68 to 4.00	Total
At solar minimum (W m^{-2})	607.75	768.25	1376.00
At solar maximum (W m^{-2})	608.75	768.35	1377.10
Percent difference	+0.164	+0.013	+0.080

lar minimum and solar maximum is 0.08%, as measured by the Earth Radiation Budget radiometer on the Nimbus 7 satellite and the Active Cavity Radiometer on the Solar Maximum Mission for solar cycle 21 (*13*).

Solar and longwave radiation that reaches the troposphere is modulated by changes in ozone concentration that occur in response to the solar cycle (*10*); the fractional ozone changes calculated in (*10*) have been used here (Table 2). The changes in total column ozone (which include those at higher altitudes not used here) are consistent with the range of 1.4 to 2.0% for the global average detected in data from the Total Ozone Mapping Spectrometer (TOMS) (*14*) over solar cycles 21 and 22, although more recent analysis of ozone data from the Solar Backscattered UltraViolet instrument (SBUV) (*15*) suggests that two-dimensional models [like that used in (*10*)] tend to underestimate the change below 16 hPa (by ~25%) and to overestimate the change above 16 hPa. Thus, the changes in ozone specified here may be too low.

The model results were analyzed so as to enable comparison with observations of apparent climate response to solar variability. First, an analysis of the high-pass transient eddy kinetic energy (EKE) at 250 hPa was carried out (Fig. 1). This field gives an indication of the strength and position of the mid-latitude storm tracks. In the Northern Hemisphere winter, there are two distinct tracks (Fig. 1A), one across the Atlantic Ocean and one across the Pacific extending into North America, whereas in the Southern Hemisphere summer, the situation is more zonally symmetric. These features correspond well to observations (*16*), although the bifurcation of the track in the eastern Atlantic noted by Brown and John (*4*) is not reproduced in the model track, which appears to correspond only to their southern route. The zonal average of Fig. 1A is shown in Fig. 1B. The zonal average difference in the EKE between runs I and IIa (solid line in Fig. 1C) shows that the Southern Hemisphere storm track has decreased on its northern side and increased on its southern side, that is, it has moved southward. The magnitude of the shift is small (~0.7° latitude or 70 km), but the overall impact is spread over most of the mid-latitude region. In the Northern Hemisphere, the effect is smaller (because it is longitudinally more variable), but the tracks over the Atlantic and eastern Pacific have moved north, again by ~70 km; this is consistent with the results of Brown and John (*4*), who showed a poleward shift of around 1° latitude in their southern route storm tracks at solar maximum. Because EKE is a measure of temporal variance, it is not easily amenable to the type of estimate of statistical significance used to analyze differences in the fields discussed below. However, when the differences in EKE between different sections of run I are compared with the difference between runs I and IIa, the probability of the peak changes happening by chance is found to be <5% for all section lengths tried (from 27 to 216 days). The difference between runs I and IIb

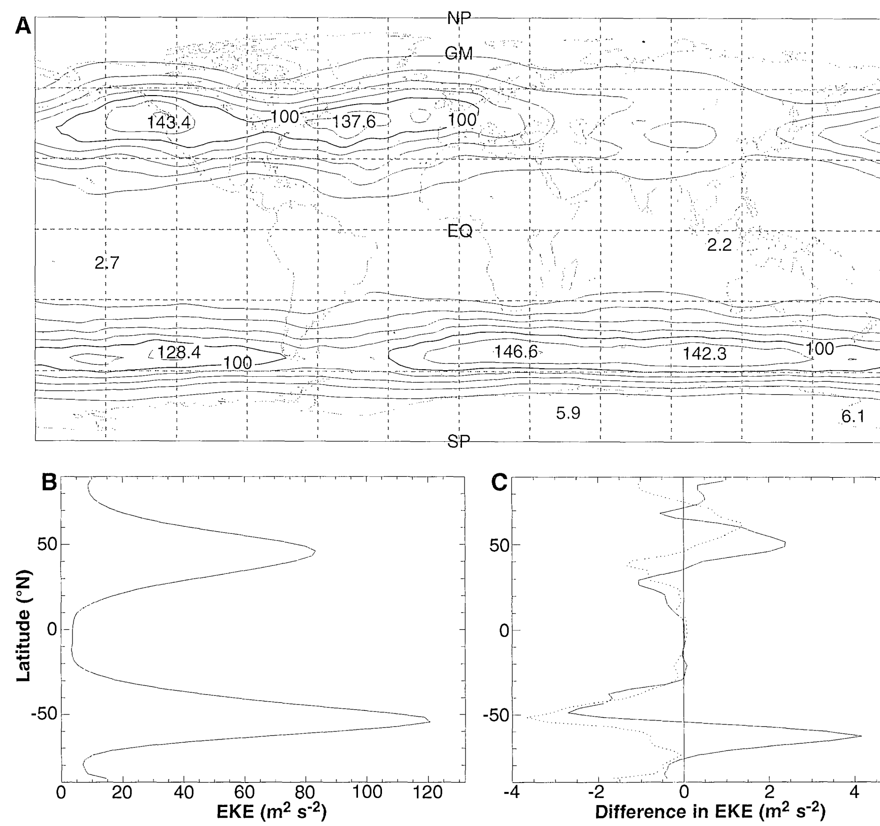

Fig. 1. Storm tracks as measured by transient EKE (m^2 s^{-2}) at 250 hPa, high-pass filtered to include only features with a time scale of ≤3 days. (**A**) Latitude-longitude plot from run I (solar minimum). NP, North Pole; ID, international date line; GM, Greenwich meridian; EQ, equator; SP, South Pole. (**B**) Zonal average of (A). (**C**) Zonal average of difference between EKE at solar maximum and solar minimum with (solid line) and without (dotted line) change in ozone.

Table 2. Percent change in ozone between runs I and IIa as a function of latitude and altitude. The change is zero elsewhere and is zonally symmetric.

Altitude (hPa)	Latitude and percent change in ozone				
	90° to 55°N	55° to 30°N	30°N to 11°S	11° to 61°S	61° to 90°S
10 to 30	2.0	2.3	2.2	2.3	2.0
30 to 50	1.8	1.8	1.7	1.7	1.4
50 to 73	1.4	1.4	1.1	1.3	1.2
73 to 103	1.1	1.0	0.6	1.0	1.0
103 to 141	0.8	0.6	0.2	0.2	0.9
Total column	1.3	1.4	1.7	1.4	1.2

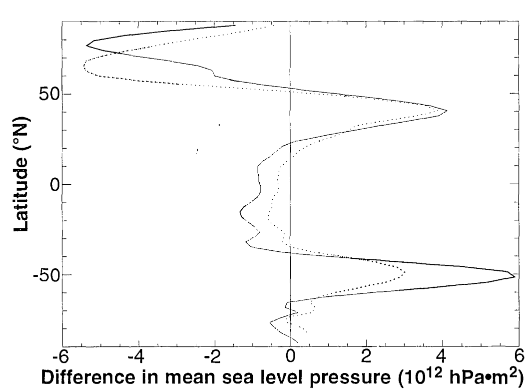

Fig. 2. Difference between solar maximum and solar minimum in area-integrated mean sea level pressure (hPa·m^2) with (solid line) and without (dotted line) change in ozone. Values have been zonally integrated in 2.79° latitude bands to reveal the relative redistribution of mass (to conserve mass, the globally integrated surface pressure must remain constant). Bold line portions indicate change that was significant at the 95% level, as calculated with Student's *t* test, taking into account the reduction in number of independent variables resulting from autocorrelation in the time series (*17*); the number of resulting degrees of freedom depends on position but was >100 in >94% of cases.

(dotted line in Fig. 1C) shows effects that are generally smaller.

Another indication of the effect of the increase in solar activity on atmospheric structure is given by the change in surface pressure (Fig. 2). The difference between runs I and IIa is a decrease of ~0.1 hPa (just significant at the 95% level) in the zonally averaged surface pressure in low latitudes and an increase of ~0.5 hPa (clearly significant at the 95% level) near 50°S, which indicates that air has moved from low to mid-latitudes. A similar increase at northern mid-latitudes is not statistically significant on the basis of the length of runs currently completed, but there does appear to be a movement away from the North Pole. The differences between runs I and IIb are similar in sense to, but generally less than half the magnitude of, those between runs I and IIa in the Southern Hemisphere.

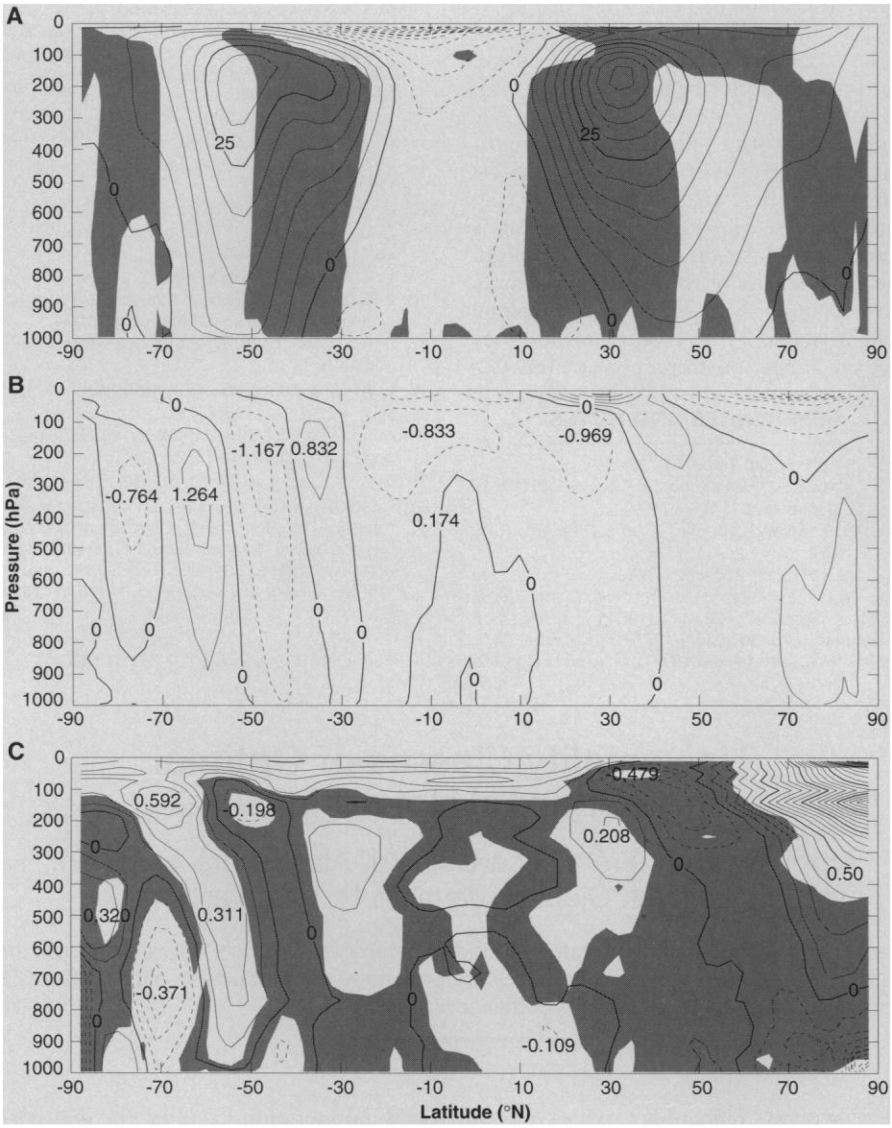

Fig. 3. Latitude-altitude plots (with altitude coordinates in hectopascals). (**A**) Zonal mean zonal wind (m s^{-1}) at solar minimum, shown by contours. Regions of descending air are shaded. (**B**) Difference in zonal mean zonal wind (m s^{-1}) between run IIa (solar maximum) and run I (solar minimum). (**C**) Difference in zonal mean temperature (kelvin) for the same runs as in (B); shaded areas are not significant at the 95% level.

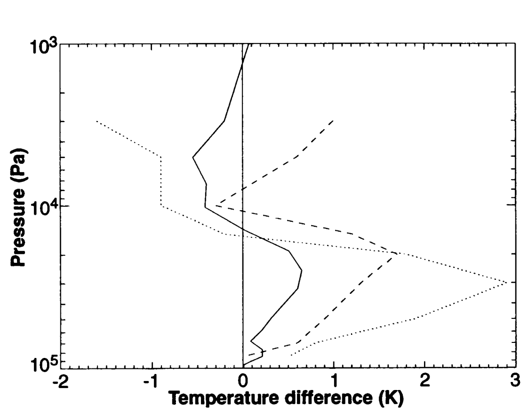

Fig. 4. Difference between solar maximum and solar minimum in temperature as a function of altitude (in hectopascals) from radiosonde data (3) at Lihue, Hawaii (22°N, 159°W), for January–February (dotted line) and November–December (dashed line) between extremes of the three solar cycles occurring between 1959 and 1994. The modeled difference between run IIa (solar maximum) and run I (solar minimum) at 30°N, 145°W is shown for mid-January (solid line). The 95% confidence limits of the model results are about ±0.25 K; uncertainty in observations is not available.

Figure 3 shows the difference between runs I and IIa in zonal mean temperature (Fig. 3C) and zonal wind (Fig. 3B) as a function of latitude and altitude. Figure 3A shows zonal mean zonal wind for run I (contours) and regions of ascent and descent (by shading). A comparison of A, B, and C of Fig. 3 suggests a cause for the changes in storm track position and surface pressure. The increases in solar UV radiation and ozone concentration cause heating in the Southern Hemisphere summer lower stratosphere (Fig. 3C). Through the thermal wind relation, this effect results in a strengthening of the summer stratosphere easterly winds, in particular of those that extend into the tropical upper troposphere, and these winds force the tropospheric westerly jets to move poleward (Fig. 3, A and B). The banding in Fig. 3B in the Southern Hemisphere is attributable to the double peak in the jet (Fig. 3A). A similar, though larger, effect is also seen in the (Northern Hemisphere only) zonal wind data analyses of Kodera (*18*). Contrary to previous theories of the response of the stratosphere-troposphere system to changes in solar activity (*7, 19*), which have concentrated on changes in the propagation of planetary waves through the stratospheric winter westerly regime, these findings suggest that changes in the Southern Hemisphere summer easterlies are important, and that ignoring changes in stratospheric ozone will limit the success of any model simulation.

The mean meridional circulation of the atmosphere is indicated by shading in Fig. 3A; the circulations involving ascent near the equator and descent in the subtropics are referred to as Hadley cells, and those in the opposite direction in mid-latitudes are called Ferrel cells. The position of the tropospheric westerly jets determines the latitudinal extent of the Hadley cells [see (*16*)]; hence, as the westerly jets move poleward at solar maximum, so do the descending portions of the Hadley cells. As a consequence, the mid-latitude storm tracks move poleward. [The dynamical mechanisms underlying this process are discussed, in a different context, by Chang (*20*).]

Vertical motion of air leads to changes

in temperature because of adiabatic compression and expansion, which result in warming during descent and cooling during ascent, respectively. Evidence for changes in the pattern of the mean meridional circulation can be seen by comparing the temperature changes (Fig. 3C) with the positions of the ascending and descending air in the control run (shading in Fig. 3A). In the middle troposphere, the cooling near 40°S is caused by the southward departure of the descending portion of the Hadley cell, and the warming around 55°S is a result of both the arrival into this region of the descending air and the southward movement of the ascending portion of the Ferrel cell. The latter then causes the extra cooling seen near 70°S.

From these results, it is evident that the vertical profiles of temperature change vary strongly with geographical position. The LvL (*2*) radiosonde data have also shown (for the boreal summer) increases at solar maximum in tropospheric temperature at low and mid-latitudes but decreases at some high-latitude stations. The temperature changes estimated by LvL (*3*) for Lihue, Hawaii (22°N, 159°W), averaged over November–December and January–February between extremes of the three solar cycles occurring between 1959 and 1994 were compared with those calculated for a near position (30°N, 145°W) in January in the present work (Fig. 4). Relative to the observational data, the model profile has a very similar structure but is smaller in magnitude. Given that the model has fixed sea surface temperatures (such that the extra solar energy reaching the surface is "lost") and that the specified ozone changes may be too low (*15*), an underestimate of the solar effects is not surprising. The only other station for which LvL show data for the boreal winter is Truk Island (7.5°N, 152°E); at this site, the observations in the troposphere showed much smaller changes in response to the solar cycle, and the model results likewise are not significantly different from zero. In the stratosphere, both the observations and the model show more warming than at Lihue. [LvL (*3*) also concluded that the shape of the temperature change profiles is consistent with changes in vertical motion.]

The model results suggest that increases in stratospheric temperature in response to enhanced solar irradiance result in stronger summer easterly winds, which penetrate into the tropical upper troposphere and force tropospheric circulation patterns poleward. The model shows changes in temperature, zonal wind, and storm track position that are similar to, although generally smaller than, those observed. The solar-induced increase in stratospheric ozone is important in determining the change in lower stratospheric temperatures and thus the subsequent climate response. There is no quasi-biennial oscillation (QBO) in the model (in effect, it is permanently in the easterly phase); hence, the claim by LvL that the QBO plays a role in modulating the impact of solar variability on the winter lower stratosphere cannot be tested. However, if the strength of the zonal wind in the tropical lower stratosphere plays an important role in transmitting the solar effects from stratosphere to troposphere, as suggested by the present results, then it is clear that modulation by the QBO is probable. The results of the model also imply that changes in stratospheric ozone brought about by any other means may have an impact on tropospheric climate.

REFERENCES AND NOTES

1. W. Herschel, *Phil. Trans.* **91**, 265 (1801).
2. K. Labitzke and H. van Loon, *J. Clim.* **5**, 240 (1992).
3. ———, *Meteorol. Z.* **3**, 259 (1994).
4. G. M. Brown and J. I. John, *J. Atmos. Terr. Phys.* **41**, 43 (1979).
5. J. Lean, *Science* **244**, 197 (1989).
6. R. Garcia, S. Solomon, G. R. Roble, D. W. Rusch, *Planet. Space Sci.* **32**, 411 (1984); L. L. Hood, *J. Geophys. Res.* **91**, 5264 (1986); S. Chandra, *Geophys. Res. Lett.* **18**, 837 (1991); T. Y. W. Huang and G. P. Brasseur, *J. Geophys. Res.* **98**, 20413 (1993); E. L. Fleming, S. Chandra, C. H. Jackman, D. B. Considine, A. R. Douglass, *J. Atmos. Terr. Phys.* **57**, 333 (1995).
7. K. Kodera, M. Chiba, K. Shibata, *Geophys. Res. Lett.* **18**, 1209 (1991).
8. D. Rind and N. K. Balachandran, *J. Clim.* **8**, 2080 (1995).
9. R. T. Wetherald and S. Manabe, *J. Atmos. Sci.* **32**, 2044 (1975); E. Nesme-Ribes, E. N. Ferreira, R. Sadourny, H. LeTruet, Z. X. Li, *J. Geophys. Res.* **98**, 18923 (1993); D. Rind and J. Overpeck, *Quat. Sci. Rev.* **12**, 357 (1993).
10. J. D. Haigh, *Nature* **370**, 544 (1994).
11. J.-J. Morcrette, *J. Geophys. Res.* **96**, 9121 (1991).
12. J. Slingo *et al., Q. J. R. Meteorol. Soc.* **120**, 881 (1994).
13. J. Lean, *Rev. Geophys.* **29**, 505 (1991).
14. L. L. Hood and J. P. McCormack, *Geophys. Res. Lett.* **19**, 2309 (1992).
15. L. L. Hood, *J. Geophys. Res.,* in press.
16. I. N. James, *Introduction to Circulating Atmospheres* (Cambridge Univ. Press, Cambridge, 1994).
17. J. A. Laurmann and W. L. Gates, *J. Atmos. Sci.* **34**, 1187 (1977).
18. K. Kodera, *J. Geophys. Res.* **100**, 14077 (1995).
19. L. L. Hood, J. L. Jirikowic, J. P. McCormack, *J. Atmos. Sci.* **50**, 3941 (1993); N. K. Balachandran and D. Rind, *J. Clim.* **8**, 2058 (1995).
20. E. K. M. Chang, *J. Atmos. Sci.* **52**, 2006 (1995).

21. I thank K. Labitzke and H. van Loon for permission to reproduce the data in Fig. 4, two anonymous referees for helpful comments, and C. Winchester for computational assistance. This work, and the UGAMP project, are supported by the UK Natural Environment Research Council.

4 August 1995; accepted 27 March 1996

Universality Classes of Optimal Channel Networks

Amos Maritan, Francesca Colaiori, Alessandro Flammini, Marek Cieplak, Jayanth R. Banavar*

Energy minimization of both homogeneous and heterogeneous river networks shows that, over a range of parameter values, there are only three distinct universality classes. The exponents for all three classes of behavior are calculated.

River networks reflect fractal properties in a power law distribution of various quantities (*1*). The striking generality of Horton's law of stream numbers (*2*) motivated Shreve (*3*) to suggest that channel networks developed in the absence of geologic controls are essentially topologically random. Nevertheless, nonrandom river networks have been consistently observed. Their existence has prompted the development of models (*2*, *4*, *5*) of drainage network optimization based on the concept of energy minimization and optimal channel networks (OCNs) (*6*, *7*). Computer simulations of homogeneous OCNs (*6*) have resulted in optimal networks with a striking similarity to those observed in nature. These results have raised the question as to whether some form of global energy minimization underlies the existence of fractal structures. Here, we solve the OCN for a range of parameters for both homogeneous and heterogeneous basins. Although we do obtain fractals, our exact results for the power law exponents do not agree with either the observational data or the computer simulations. The disagreement between the results of our analytic solution and the computer simulations (*6*) is a result of the fact that the latter were only able to access a set of local minima (which depend-

A. Maritan, F. Colaiori, A. Flammini, Istituto Nazionale di Fisica della Materia, International School for Advanced Studies, I-34014 Grignano di Trieste and sezione INFN di Trieste, Italy.

M. Cieplak, Institute of Physics, Polish Academy of Sciences, 02-668 Warsaw, Poland.

J. R. Banavar, Department of Physics and Center for Materials Physics, The Pennsylvania State University, 104 Davey Laboratory, University Park, PA 16802, USA.

*To whom correspondence should be addressed.